

PAPER

CrossMark
click for updatesCite this: *J. Mater. Chem. A*, 2015, 3,
10127Received 13th January 2015
Accepted 2nd April 2015

DOI: 10.1039/c5ta00286a

www.rsc.org/MaterialsA

Long-life, high-efficiency lithium/sulfur batteries
from sulfurized carbon nanotube cathodes†Jianhua Yan,^{ab} Xingbo Liu,^b Xianfeng Wang^a and Bingyun Li^{*a}

The long-term cycling properties of Li–S cells comprised of sulfurized carbon nanotubes (SCNTs) were thoroughly investigated. A high concentration (68 wt%) of sulfur was successfully immobilized on the surfaces of functionalized CNTs using a unique fabrication method that combined solvent exchange and surface and low-temperature treatments. The developed Li–S cells presented a long cycle life exceeding 1300 cycles and an extremely low capacity decay rate (0.025% per cycle) at 1/3 C rate. Moreover, these Li–S cells had an excellent high-rate response up to 2 C with high Coulombic efficiency (above 95.5%) and high sulfur utilizations (1180 mA h g⁻¹ of sulfur over 300 cycles at 0.25 C, 799 mA h g⁻¹ over 600 cycles at 0.75 C, 810 mA h g⁻¹ over 500 cycles at 1 C, and 400 mA h g⁻¹ over 500 cycles at 2 C). These results provide important progress towards understanding the role of SCNTs in developing Li–S batteries with potentially high efficiency and long-term service life.

Introduction

Rechargeable Li–S batteries have attracted significant attention due to their high specific energy.¹ They are promising candidates for applications in electric vehicles and grid-level energy storage. However, their inferior cycle performance, low sulfur utilization, and low Coulombic efficiency are the major technical obstacles, mainly due to the insulating nature of sulfur (5×10^{-30} S cm⁻¹) and the high solubility of intermediate long-chain lithium polysulfides (Li₂S_n, $n \geq 4$) in liquid electrolytes thereby resulting in parasitic reactions with the Li-anode.^{2–5} In addition, the detachment of polar lithium polysulfides from nonpolar conductive carbon matrices during charge/discharge processes may contribute to fast capacity decay.^{6,7} Various sulfur carbon composites^{6–11} or electrolyte additives¹² have been studied in order to enhance the conductivity and stability of sulfur cathodes. However, these strategies may only slow down the dissolution of polysulfides in a short term, because the physical barriers provided by carbon matrices cannot prevent the migration of polar polysulfide anions, which are driven by an electrical field in electrolytes.

As a promising cathode material, sulfurized carbons (SCs) have been intensively investigated due to their ability to chemically trap polysulfides and thereby may potentially reduce the dissolution of polysulfides as well as the parasitic reactions

with Li-anodes.^{13–15} Commonly, SCs are synthesized at high temperatures (>500 °C) by reacting carbon with sulfur. During the reaction, S₈ may decompose into small sulfur allotropes (*i.e.*, S₂, S₄, and S₆) which can bond with carbon atoms *via* reacting with surface functional groups on carbon surfaces.¹⁴ Researchers have studied various carbon or polymer materials that contain surface functional groups such as –OH, >C=O, –C(=O)OH, and >C=C<, which have shown some progress in binding sulfur on the surfaces of carbon during heat treatments.^{16–20} Indeed, SCs have been shown to reduce the adverse effects of polysulfide dissolution, but at the same time, have caused several concerns including: (i) the low sulfur content (*e.g.* <50 wt%), caused by high-temperature treatments (*e.g.* >500 °C), has reduced the energy density of Li–S batteries. The significant use of conductive agents may also neutralize the high energy density of Li–S batteries. For example, Zhang *et al.* reported sulfurized carbon fibers with a capacity of only 288 mA h g⁻¹ at the 50th cycle.¹⁸ (ii) Long sulfur chains (–S_x–, $x > 4$) bonded on carbon have led to high capacities but inferior cycling stability, since they can rearrange to release elemental sulfur and form soluble polysulfides during cell operations, whereas short sulfur chains (–S_x–, $x \leq 4$) may result in low capacity but good capacity retention. Therefore, it is important to develop appropriate sulfurization technology of SC cathodes to enhance sulphur immobilization and utilization in Li–S batteries.

Herein, we report long-life and high-efficiency Li–S cells comprised of sulfurized carbon nanotube (SCNT) cathodes. We developed a new strategy to fabricate SCNT materials with a high content (68 wt%) of sulfur under a relatively low temperature of 300 °C, by functionalizing CNTs and using a solvent exchange method²¹ to graft sulfur chains onto CNTs. CNT was

^aBiomaterials, Bioengineering & Nanotechnology Laboratory, Department of Orthopaedics, West Virginia University, Morgantown, West Virginia 26506, USA. E-mail: bili@hsc.wvu.edu

^bDepartment of Mechanical and Aerospace Engineering, West Virginia University, Morgantown, West Virginia 26506, USA

† Electronic supplementary information (ESI) available. See DOI: 10.1039/c5ta00286a

chosen as a sulfur carrier, because it is composed of hybridized sp^2 carbon that could form electrochemically active C–S bonds.^{22,23} CNT also has superior mechanical strength and electrical conductivity. In addition, CNT has tunable chemical characters including formation of oxygen-containing groups on surfaces and changes in nanotube structures and thermal stability; these chemical characters may enhance the reactivity of aromatic carbon rings for sulfur immobilization *via* forming covalent bonds (e.g., O–S bonds) or holding sulfur in nanopores of CNTs.^{24–27} As a result, Li–S cells comprised of SCNT cathodes exhibited an ultralong cycle life (exceeding 1300 cycles at 1/3 C) with an ultrahigh capacity retention (67.8% from 809 to 549 mA h g^{-1} over 1300 cycles). Moreover, these Li–S cells had an excellent high-rate response up to 2 C, and their Coulombic efficiency was higher than 95.5%.

Experimental

Synthesis of SCNTs

Our strategy for the preparation of SCNT materials with a high content of sulfur involved CNT surface treatment and solvent exchange methods. Detailed synthesis procedures are described in the ESI.† The typical fabrication process of the SCNT materials is shown in Fig. 1a and b. CNTs were firstly refluxed in a mixture of concentrated nitric acid and sulfuric acid to remove amorphous carbon and to form oxygen-containing groups on CNT surfaces. Next, CNTs were treated with hydrogen peroxide (H_2O_2), and sulfur dissolved in carbon disulfide (CS_2) solution was then added dropwise to form pristine SCNTs. During such a process, CS_2 quickly reacted with H_2O_2 and formed colloidal sulfur.²⁸ Lastly, the samples were treated at 300 °C in a vacuum oven for 5 h, and designated as SCNT-300. Two types of control samples were prepared: (i) SCNT-159, obtained by heating the pristine SCNTs in a vacuum oven at 159 °C for 10 h; (ii) S/CNT-159, fabricated by mixing sulfur and functionalized CNTs together and heating the mixture in a vacuum oven at 159 °C for 10 h.

Electrochemical tests

Cathode slurries were prepared by mixing 90 wt% of SCNTs and 10 wt% of polyvinylidene fluoride (PVDF), and then coated onto aluminum foils that had been pre-coated with a thin layer of carbon. The electrodes were dried at 60 °C in a vacuum oven for

5 h. The electrochemical performance of the SCNT electrodes was evaluated by measuring coin-type half-cells with lithium foil as the counter electrodes. CR2016-type cells were assembled in an argon glove box. 1.0 mol L^{-1} lithium bis(trifluoromethane sulfonyl) imide (LiTFSI) and 0.15 mol L^{-1} $LiNO_3$ dissolved in dioxolane (DOL) and dimethoxyethane (DME) (1 : 1, v/v) were used as electrolytes and Cellgard 2400 microporous membranes were used as separators. The cathode material was on a 0.8 cm \times 0.8 cm square aluminium substrate, and the amount of electrolyte for each cell was about 0.02 mL. The cells were charged and discharged at different current rates between 1 (or 1.5) and 3 V (*vs.* Li/Li⁺) using an Arbin battery test station. The cyclic voltammetry (CV) measurements were carried out with a scan rate of 0.05 $mV s^{-1}$ on a NOVA potentiostat analyzer. The specific capacity was calculated based on active sulfur materials. All experiments were conducted at room temperature unless specified.

Results and discussion

Characterization of SCNT

After being treated in concentrated nitric acid and sulfuric acid followed by H_2O_2 , CNTs were found to have much more surface active groups (19.7 wt%) (Fig. S1a, b, Tables S1 and S2†) and much lower thermal stability (Fig. S1c†) compared to the pristine CNTs.²⁹ The morphologies of the CNTs before (Fig. 2a) and after (Fig. 2b) H_2O_2 treatment were similar but the CNTs tended to be more agglomerated after H_2O_2 treatment. Sulfur was well dispersed on the CNT surfaces after the solvent-exchange process (Fig. 2c), probably because the reactive groups on CNT surfaces might act as growth points for sulfur precipitation. After being treated at 300 °C for 5 h, most of the bulk sulfur was evaporated and a dense thin layer of sulfur was formed on CNT surfaces (Fig. 2d). The synthesized SCNTs tended to agglomerate due to van der Waals interactions and formed 3D interconnected ionic- and electric-conductive channels. Meanwhile, sulfur particles were observed mainly at the ends of CNTs (Fig. 2e and f), which was probably due to the strong capillary force at the ends of CNTs.

The sulfur content and the mechanism of sulfur incorporation in SCNTs were examined using thermo-gravimetric analysis (TGA). The weight contents of sulfur in SCNT-159 and SCNT-300 were found to be 84.8% (or 3.07 $mg cm^{-2}$) and 68.0%

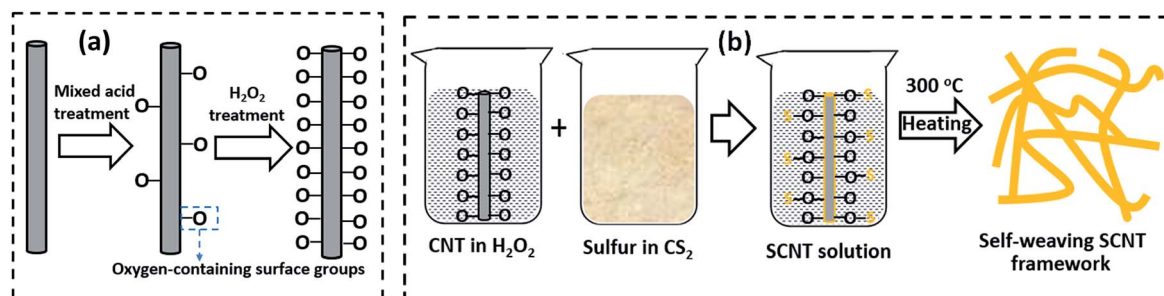


Fig. 1 Synthesis and characterization of SCNT composites. Schematic illustrations of (a) the proposed treatment for integrating oxygen-containing surface groups into CNTs and (b) the proposed strategy for grafting sulphur onto CNTs.

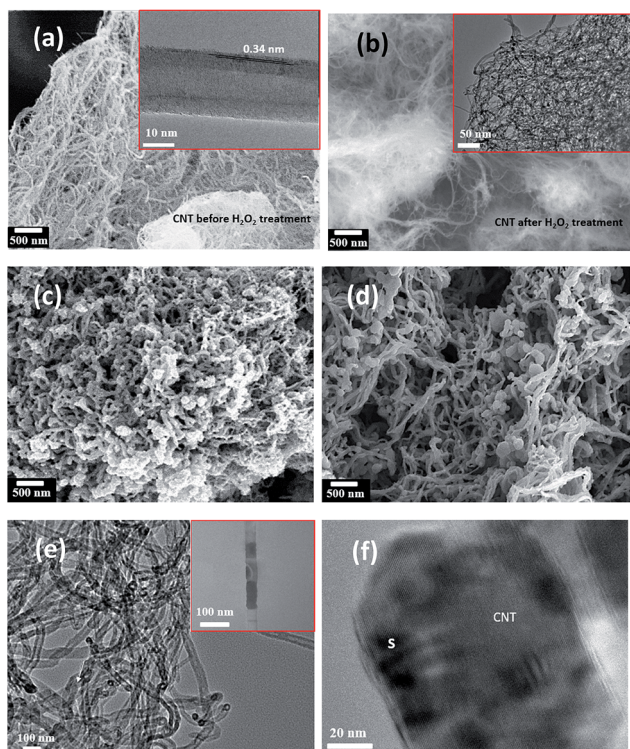


Fig. 2 Characterization of SCNTs and related materials. Typical morphologies of CNTs (a) before and (b) after H_2O_2 treatment. Inset transmission electron microscopy (TEM) figures are with high magnification. Typical morphologies of SCNT (c) before and (d) after heat treatment. (e and f) TEM images of SCNT materials after heat treatment.

(or 2.94 mg cm^{-2}), respectively (Fig. 3a and Table S3†). The weight loss of SCNT-300 could be distinctly divided into two regions according to the rates of weight loss: The fast weight loss region from 300 to 400 °C probably belonged to the decomposition of S–S bonds, and the slow weight loss region from 400 to 700 °C could be assigned to the breakdown of C–S bonds. It is known that the C–S bond has a much higher bond energy than the S–S bond (*i.e.*, 740 kJ mol^{-1} for C–S and 418 kJ mol^{-1} for the S–S bond at 298 K).³⁰

The structural characteristics of the prepared CNTs and SCNTs were examined using Fourier transform infrared spectroscopy (FTIR), as shown in Fig. 3b. Both the pristine CNTs and the prepared CNTs had typical characteristic peaks at 1290, 1430, and 1680 cm^{-1} corresponding to C–O, C=O, and C=C stretches, respectively.³¹ The spectra of SCNTs were much different from those of CNTs. For both SCNT-159 and SCNT-300, the C–O stretching vibration at 1290 cm^{-1} was shifted to lower wave lengths and the intensity of both C=C and C=O vibrational bands at 1680 and 1439 cm^{-1} , respectively, were significantly weak, indicating the replacement of H and O atoms by S atoms. In addition, a new band appeared at 1050 cm^{-1} for SCNT-159 and SCNT-300, which could be ascribed to the vibrations of O–S. A second new band, centered at 925 cm^{-1} for SCNT-300, could be assigned to the vibrations of C–S.^{32,33} Both the TGA and FTIR results indicated that a large

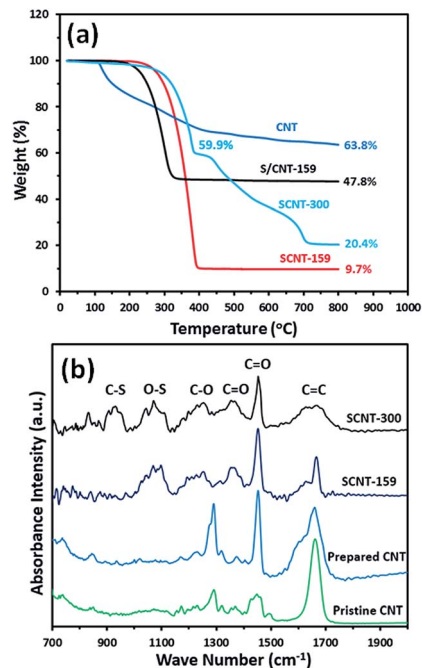


Fig. 3 Characterization and the proposed structure of SCNT cathodes studied. (a) TGA profiles of CNT, S/CNT-159, SCNT-159, and SCNT-300. The tests were performed in a nitrogen environment with a heating rate of 5 °C min^{-1} . (b) FTIR spectra of pristine CNT, the prepared CNT, SCNT-159, and SCNT-300.

portion of elemental sulfur reacted with CNTs and formed a cross-linked porous SCNT framework with short sulfur chains ($-\text{S}_x-$). As a result, the majority of sulfur in SCNTs had the uncommon monoclinic phase rather than the typical orthorhombic phase, and the monoclinic sulfur was very stable even after being stored for 30 days at room temperature (Fig. S2†).

The presence of C–S and O–S bonds was further examined using X-ray photoelectron spectroscopy (XPS) (Fig. 4). The S 2p spectra of SCNT-300 were composed of three sub-peaks (Fig. 4b). The peak at 164.2 eV in the S 2p_{3/2} spectrum corresponded to elemental sulfur. An additional peak at 163.8 eV in the S 2p_{3/2} spectrum was slightly lower than that of elemental sulfur, revealing the possible presence of the S–C species.³⁴ The peak at 165.4 eV in the S 2p_{1/2} spectrum suggested that S atoms were linked to a carbon ring or oxygen atoms. Fig. 4c and d show the XPS spectra of the C 1s for the prepared CNTs and SCNT-300, respectively. Compared to CNT, the C–O and C=O peaks of SCNT-300 shifted to higher binding energies. The tip-shift of these two peaks, due to the polar characters of the carbon sulfur and oxygen sulfur bonds, was an evidence of the incorporation of sulfur into the CNT framework. Fig. 4e and f show the XPS spectra of the O 1s core level of the prepared CNTs and SCNT-300, respectively. Both of the two spectra could be separated and fitted into two peaks. The lower binding energy feature (532.2 eV) was due to C=O groups in the aromatic ring. The second peak was due to C–O bonds.

Fig. 5a shows the first two charge/discharge curves of SCNT-300 cathodes at 0.75 C. Three discharge plateaus were clearly observed at 2.3, 2.1, and 1.9 V. Plateau I was believed to be

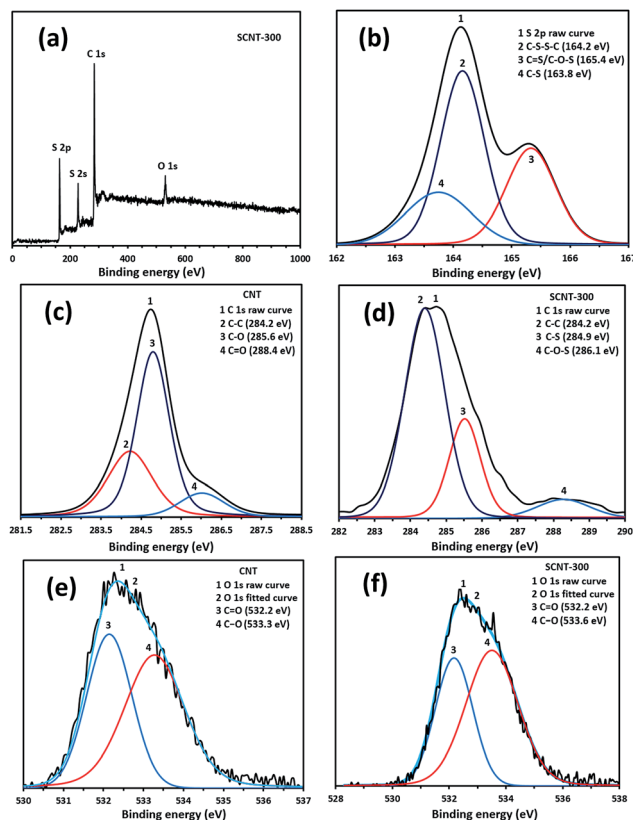


Fig. 4 XPS analysis of functionalized CNTs and SCNT-300. (a) Wide range spectrum of SCNT-300. (b) XPS data of S 2p regions of SCNT-300. XPS data of C 1s regions of (c) CNT and (d) SCNT-300. XPS data of O 1s regions of (e) CNT and (f) SCNT-300.

related to the reduction of S_8 to high-order soluble lithium polysulphides (*i.e.*, Li_2S_4), and plateau II was due to further reduction of Li_2S_4 into Li_2S . While plateau III at 1.9 V was lower than the potential of S_4^{2-} to Li_2S_2 reaction at around 2.1 V. This third discharge plateau was probably related to the reduction of short sulphur chains that covalently bonded on CNTs. Generally, the Li-S cells comprised of sulfurized carbon cathodes featured a single discharge plateau between 2 and 1.6 V.¹⁵ The reverse reactions of SCNT-300 cathodes in the oxidation process also had three potential plateaus in the charge curve. It seems that the SCNT-300 presented both behaviors of elemental sulfur and sulfur bonded on CNT surfaces. As a comparison, we examined the voltage profiles of SCNT-159 cathodes (Fig. 5b), which had typical sulfur cathode charge and discharge behaviors with two discharge potential plateaus at 2.35 and 2.1 V, and two charge potential plateaus at 2.38 and 2.40 V.

The CV tests of SCNT-300 and SCNT-159 cathodes were performed between 3.0 and 1.0 V using a 0.05 mV s^{-1} scan rate. For SCNT-300, three reduction and three oxidation peaks were observed (Fig. 5c), indicating that the electrochemical reactions in SCNT-300 were dominated by a new reaction, represented by the oxidation peak at 2.1 V and the third reduction peak at 1.9 V. It seems that the intermediate reactions of sulfur and polysulfides in conventional cathodes were suppressed in the SCNT-300 cathodes. In comparison, in the CV curves (Fig. 5d) of SCNT-

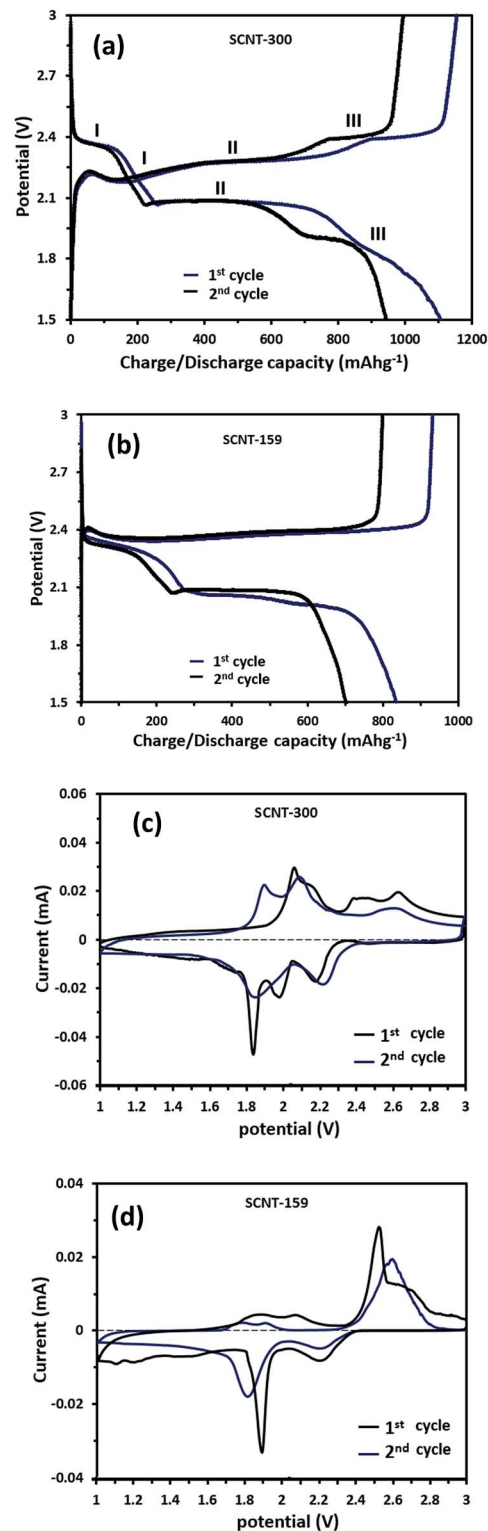


Fig. 5 Electrochemical performance of Li-S cells comprised of SCNT cathodes. Voltage profiles of the first two charge/discharge cycles of Li-S cells containing (a) SCNT-300 cathodes and (b) SCNT-159 cathodes at a current density of 0.75 C ($1 \text{ C} = 1675 \text{ mA g}^{-1}$). CV curves of Li-S cells containing (c) SCNT-300 cathodes and (d) SCNT-159 cathodes at a scan rate of 0.05 mV s^{-1} at the first two cycles.

159 cathodes, two partially overlapped oxidation peaks centered at 2.05 V were observed, in addition to the two typical sulfur oxidation peaks at 2.5 and 2.6 V. The new oxidation peaks of SCNT-159, which were not treated at 300 °C, could be caused by O–S bonds, since multiple studies^{35–37} showed that chemical reactions between sulfur or polysulfides and oxygen functional groups on CNTs could occur and lead to improved stability of Li–S cells. In addition, the wide cathodic base line from 1.5–1 V might be due to the reduction of oxygen-containing surface groups or the reduction of the electrolyte additives of lithium nitrite.³⁸

SCNT-300 cathodes were found to present a great rate capability (Fig. 6a). With the current density varying from 0.25 to 2 C, the SCNT-300 cathodes exhibited a high participation of sulfur and preserved decent capacity retentions over long cycling. For instance, at 0.25 C, the initial discharge capacity reached 1002 mA h g⁻¹, which was 59.8% of the theoretical value of sulfur. A quick increase in discharge capacities was

observed in the first 5 cycles followed with a gradual decrease in the following 35 cycles. After that, the cathode reached a steady state and exhibited a stable lithiation degree with a reversible capacity of 1180 mA h g⁻¹ with almost 100% capacity retention even after 300 cycles.

The cycling behavior and Coulombic efficiency of Li–S cells comprised of SCNT-300 cathodes at different current densities are shown in Fig. 6b. Excellent cycling stabilities were observed at relatively lower rates (0.25 C, 0.75 C and 1 C). For instance, at 0.75 C, the cell exhibited an initial discharge capacity of 1291 mA h g⁻¹, corresponding to 77.1% of sulfur participating in reactions. The cell showed a great stability of 67.5% retention with a discharge capacity of 799 mA h g⁻¹ over 600 cycles except the 1st cycle. In addition, the Coulombic efficiency of the cells was always higher than 95.5%, indicating the effectiveness of SCNT-300 cathodes in trapping intermediate lithium polysulfides during discharge processes. However, at a relatively higher rate of 2 C, the SCNT-300 cathodes had a fast capacity fading of 39% retention after 500 cycles. At such a high current rate, sulfur might not react completely and the cathode might have a severe polarization, which could inhibit regular lithium intercalation/de-intercalation processes. The discharge curve at 2 C demonstrated a severe voltage hysteresis with a shortened capacity in comparison with those in lower current rates (Fig. S3†), and only the first discharge plateau was observed in the later charge/discharge cycles (Fig. S4†).

SCNT-300 cathodes were also cycled up to 1300 cycles at a rate of 1/3 C and were found to present an extremely low capacity decay rate (0.025% per cycle) (Fig. 6c). After 1300 cycles, the discharge capacity was 549 mA h g⁻¹ of sulfur. When calculating the capacity with the whole cathode weight, the retained discharge capacity of the Li–S cells over 1300 cycles was 336 mA h g⁻¹, which was still much higher than currently commercialized Li-ion batteries. In contrast, the Li–S cells containing SCNT-159 cathodes had a fast capacity fading of only 30.7% retention from 1095 (in the 6th cycle) to 336 mA h g⁻¹ over 600 cycles with a relatively low average Coulombic efficiency of 87.1% (Fig. S5†). The capacity at 1/3 C was smaller than that at 1 C and the underlying reason is still unknown and will be investigated in the future.

Compared to the performance of recently reported S-doped CNT cathodes,^{39–43} the SCNT-300 cathodes had much higher capacity retention and much higher capacity utilization at 1 C. The capacity utilization of SCNT-300 cathodes was also higher than that of composite electrodes at C/10 and C/20 rates.^{42,43} Such enhanced performance likely originated from the good dispersion of S within the CNT matrices, good mechanical stability of cathodes, and suppressed polysulfide dissolution. Specifically, the SCNT-300 cathodes enhanced the electrochemical performance of Li–S cells in the following three aspects: (i) The as-prepared CNTs tended to agglomerate to form a strong skeleton with a porous 3D structure that could provide interconnected channels for the transport of electrons and ions. Being treated with the concentrated acids and H₂O₂ these CNTs had many nanopores and multiple surface reactive groups, which could react with sulfur in the subsequent synthesis process. To verify the strong affinity between sulfur

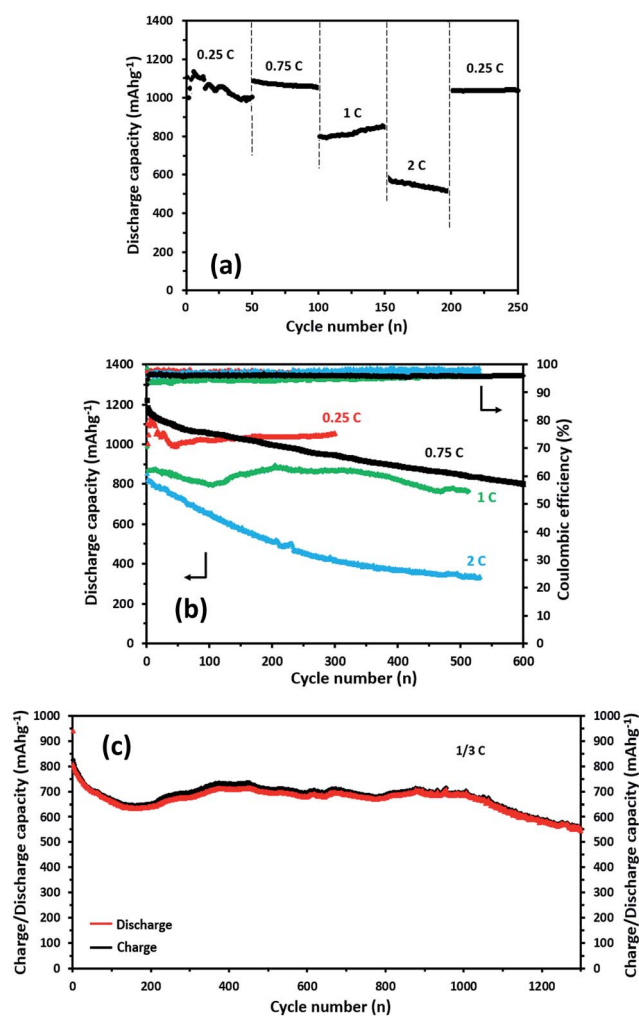


Fig. 6 Electrochemical performance of Li–S cells comprised of SCNT-300 cathodes. Capacities were normalized by the mass of sulfur. (a) Rate performance. (b) Cycling performance and Coulombic efficiency at different rates. (c) Long-term cycling tests at the 1/3 C rate.

and CNTs, we tested the performance of Li-S cells employing S/CNT-159 cathodes, in which CNTs were not treated with the concentrated acid mixture of nitric acid and sulfuric acid or treated with H₂O₂ solution. The results were shown in Fig. S6.† Clearly, both capacity and Coulombic efficiency of S/CNT-159 cathodes were worse than those of SCNT-159 and SCNT-300, indicating the advantages of combining solvent exchange and surface treatment with low-temperature treatment. (ii) The proposed synthesis method for SCNT-300 materials had great advantages such as high sulfur immobilization and low temperature treatment. The surface treatment and solvent exchange processes were crucial for high sulfur immobilization and improved the interactions between sulfur and CNTs. The heat-treatment process was also important since it allowed molten sulfur to be immobilized onto CNTs through nanopores and to form C-S bonds. (iii) The C-S bonds resulted in enhanced utilization of sulphur, and suppressed the dissolution of polysulfides into liquid electrolytes. In addition, the oxygen-containing surface groups improved the interactions of CNT with sulfur and enhanced the physical and chemical sorptions of sulfur particles and polysulfide anions during cell operation.

Conclusions

To summarize, SCNT-300 cathodes with a high sulfur content of 68 wt% were fabricated by combining surface treatment and solvent exchange methods. SEM and TEM images indicated that dense sulfur layers were formed onto CNT surfaces with the help of H₂O₂ and CS₂ as the two reaction solutions for sulfur precipitation. The interconnected 3D CNT framework served as an electrical conductive network and could accommodate high amounts of sulfur. As a result, the SCNT-300 cathodes demonstrated high performance and cyclic stability with high Coulombic efficiency for Li-S batteries.

The authors declare no competing financial interest.

Acknowledgements

The authors acknowledge the use of WVU Shared Research Facilities and financial support from the WVHEPC (West Virginia Higher Education Policy Commission) Division of Science and Research. We appreciate the assistance of Weiqiang Ding, Ph.D., in collecting XPS and XRD data. We thank Suzanne Danley for proofreading.

References

- 1 J. Yan, X. Liu and B. Li, *RSC Adv.*, 2014, **4**, 63268.
- 2 P. G. Bruce, S. A. Freunberger, L. J. Hardwick and J. M. Tarascon, *Nat. Mater.*, 2012, **11**, 19.
- 3 J. M. Tarascon and M. Armand, *Nature*, 2001, **414**, 359.
- 4 C. Tang, Q. Zhang, M. Zhao, J. Huang, X. Cheng, G. Tian, H. Peng and F. Wei, *Adv. Mater.*, 2014, **26**, 6100.
- 5 Y. Yang, G. Y. Zheng and Y. Cui, *J. Chem. Soc. Rev.*, 2013, **42**, 3018.
- 6 G. Zheng, Q. Zhang, J. J. Cha, Y. Yang, W. Li, Z. She and Y. Cui, *Nano Lett.*, 2013, **13**, 1265.
- 7 Z. Wang, Y. Dong, H. Li, Z. Zhao, H. Wu, C. Hao, S. Liu, J. Qiu and X. Lou, *Nat. Commun.*, 2014, **5**, 5002.
- 8 Y. Su and A. Manthiram, *Nat. Commun.*, 2012, **3**, 1166.
- 9 H. Wang, Y. Yang, Y. Liang, J. T. Robinson, Y. Li, A. Jackson, Y. Cui and H. Dai, *Nano Lett.*, 2011, **11**, 2644.
- 10 B. Zhang, X. Qin, G. R. Li and X. P. Gao, *Energy Environ. Sci.*, 2010, **3**, 1531.
- 11 M. K. Song, Y. Zhang and E. J. Cairns, *Nano Lett.*, 2013, **13**, 5891.
- 12 L. Suo, Y. Hu, H. Li, M. Armand and L. Chen, *Nat. Commun.*, 2014, **4**, 1481.
- 13 J. S. Park, G. B. Cho, H. S. Ryu, J. H. Ahn and K. W. Kim, *Mater. Technol.*, 2013, **28**, 270.
- 14 S. Evers and L. F. Nazar, *Acc. Chem. Res.*, 2013, **46**, 1135.
- 15 S. S. Zhang, *Front. Energy Res.*, 2013, **1**, 10.
- 16 S. Xin, L. Gu, N. Zhao, Y. Yin, L. Zhou, Y. Guo and L. Wan, *J. Am. Chem. Soc.*, 2012, **134**, 18510.
- 17 J. Fanous, M. Wegner, M. S. Spera and M. R. Buchmeiser, *Electrochem. Soc.*, 2013, **160**, A1169.
- 18 W. Zhang, D. Qiao, J. Pan, Y. Cao, H. Yang and X. Ai, *Electrochim. Acta*, 2013, **87**, 497.
- 19 B. Duan, W. Wang, A. Wang, K. Yuan, Z. Yu, H. Zhao, J. Qiu and Y. Yang, *J. Mater. Chem. A*, 2013, **1**, 13261.
- 20 J. Wang, J. Yang, C. Wan, K. Du, J. Xie and N. Xu, *Adv. Funct. Mater.*, 2013, **13**, 487.
- 21 Y. Yeo, A. U. Chen, O. A. Basaran and K. Park, *Pharm. Res.*, 2004, **21**, 8.
- 22 J. Guo, Y. Xu and C. Wang, *Nano Lett.*, 2011, **11**, 4288.
- 23 L. Xiao, Y. Cao, J. Xiao, B. Schwenzer, M. H. Engelhard, L. Saraf, Z. Nie, G. J. Exarhos and J. Liu, *Adv. Mater.*, 2012, **24**, 1176.
- 24 D. Tasis, N. Tagmatarchis, A. Bianco and M. Prato, *Chem. Rev.*, 2006, **106**, 1105.
- 25 M. F. Volder, S. H. Tawfick, R. H. Baughman and A. J. Hart, *Science*, 2013, **339**, 535.
- 26 Z. Fan, J. Yan, L. Zhi, Q. Zhang, T. Wei, J. Feng, M. Zhang, W. Qian and F. Wei, *Adv. Mater.*, 2010, **22**, 3723.
- 27 J. Chen, X. Jia, Q. She, C. Wang, Q. Zhang, M. Zheng and Q. Dong, *Electrochim. Acta*, 2010, **55**, 8062.
- 28 Y. G. Adewuyi and G. R. Carmichael, *Environ. Sci. Technol.*, 1987, **21**, 170.
- 29 Y. Peng and H. Liu, *Ind. Eng. Chem. Res.*, 2006, **45**, 6483.
- 30 S. S. Zhang, *Energy*, 2014, **7**, 4588.
- 31 B. P. Vinayan, R. Nagar, V. Raman, N. Rajalakshmi, K. S. Dhathathreyan and S. Ramaprabhu, *J. Mater. Chem.*, 2012, **22**, 9949.
- 32 X. Yu, J. Xie, J. Yang, H. Huang, K. Wang and Z. S. Wen, *J. Electroanal. Chem.*, 2004, **573**, 121.
- 33 B. Meyer, *Chem. Rev.*, 1976, **76**, 367.
- 34 M. S. Park, J. Yu, K. Kim, G. Jeong, J. Kim, Y. Jo, U. Hwang, S. Kang, T. Woo and Y. Kim, *Phys. Chem. Chem. Phys.*, 2012, **14**, 6796.
- 35 J. Song, T. Xu, M. Gordin, P. Zhu, D. Lv, Y.-B. Jiang, Y. Chen, Y. Duan and D. Wang, *Adv. Funct. Mater.*, 2014, **24**, 1243.

- 36 P. Zhu, J. Song, D. Lv, D. Wang, C. Jaye, D. A. Fischer, T. Wu and Y. Chen, *J. Phys. Chem. C*, 2014, **118**, 7765.
- 37 S. Xin, L. Gu, N. Zhao, Y. Yin, L. Zhou, Y. Guo and L. Wan, *J. Am. Chem. Soc.*, 2012, **134**, 18510.
- 38 S. W. Lee, N. Yabuuchi, B. M. Gallant, S. Chen, B. Kim, P. T. Hammond and S. Yang, *Nat. Nanotechnol.*, 2010, **5**, 531.
- 39 Y. Li, R. Mi, S. Li, X. Liu, W. Ren, H. Liu, J. Mei and W. M. Lau, *Int. J. Hydrogen Energy*, 2014, **39**, 16073.
- 40 Y. Su and A. Manthiram, *Chem. Commun.*, 2012, **48**, 8817.
- 41 Y. Fu, Y. Su and A. Manthiram, *Angew. Chem., Int. Ed.*, 2013, **52**, 6930.
- 42 X. Cheng, J. Huang, Q. Zhang, H. Peng, M. Zhao and F. Wei, *Nano Energy*, 2014, **4**, 65.
- 43 Z. Yuan, H. Peng, J. Huang, X. Liu, D. Wang, X. Cheng and Q. Zhang, *Adv. Funct. Mater.*, 2014, **24**, 6105.